POLISH MARITIME RESEARCH Special Issue 2018 S2 (98) 2018 Vol. 25; pp. 85-91
10.2478/pomr-2018-0078

# RESEARCH ON RUB-IMPACT LOADS RESPONSE OF SHIP SHAFTING

**DONG Liang-xiong, associate Prof. Dr.**
**SHI Yi-ran, Master.**
**WANG Shao-hua, Master.**
Zhejiang Ocean University, Zhoushan, Zhejiang, China

**ABSTRACT**

*The anti-impact ability of shafting affects stability and security of the ship power transmission directly. Moreover, it also cannot be ignored that the rub-impact loads have influence on the torsion vibration of ship shafting. In order to solve the problem of engineering application of reliability assessment under rub-impact loads, a test rig with rubbing generator is established. By carrying out the integrative analysis, the torsional vibration characteristics, such as vibration amplitude and orbit of axle center under the rub impact load are studied. According to the rub-impact conditions obtained through numerical simulation, the experimental verification is carried out on the test rig with rubbing generator. The results show that it is not obvious the influence of rub-impact loads upon the shafting torsion vibration except in special working conditions, that can be simulated by the rubbing generator. The maximum amplitude of torsional vibration is influenced by the radial rigidity as well as the friction coefficient of rubbing body, and the degree of influence is difference under conditions of continuous rubbing and serious rubbing. By adjusting the rigidity of stern bearing, the influence of rub-impact upon shafting can be weaken, which provides a theoretical reference for the safety evaluation of ship shafting.*

**Keywords:** rub-impact; Torsional Vibration; Test Rig; Rubbing Generator

## INTRODUCTION

The tail shaft is an important part of the marine propulsion system. The stern tube bearing supports not only its own gravity but also the weight of the propeller and thus withstands the largest load of the ship shafting. With the increasing scale of ship, the increasing hull deformation have generated many troubles of mutually affect between the ship shafting and hull structure. Besides, subjected to various wave loads, the ship shafting work under transient conditions such as variable load or variable inertia, which produce certain influence to the dynamic characteristics of propulsion system [1]. During the running of the ship shaft, as the ship shafting misalignment or bending, the vibration amplitude of the stern shaft will be augmented. When the amplitude exceeds the gap between the bearing and the journal, the collision and friction between them will happen that are known as the rub-impact [2]. Rub-impact is one common phenomenon of large-scale rotating machinery that will wear the stern tube bearing, cause increase of the gap between bearing and journal, even lead to failure of propulsion system and then affect the safe operation of ship [3].

In order to study the rub-impact phenomenon, the test rig is generally adopted for experimental research. However, the phenomenon of rub-impact between journal and bearing under different marine environment are very complex [4],

and the effectiveness of the experimental research depends on the similarity between the working condition of the test rig and that of actual ship.

In this study, a mass-spring model was proposed for stern structure modeling, and the equivalent mechanical models of spring-vibrator-damper were given by mechanical equivalent principle. Considering the test of rub-impact is destructive, a rubbing generator is adopted to simulate rub-impact load between the tail shaft and the bearing [5]. And then, a variety of conditions of rub-impact load can be realized by adjustment of rubbing generator. By analyzing the rub-impact induced vibration response in both test rig and real ship, the influence of rubbing loads upon ship shafting can be obtained. The study can play a guiding role in solving practical engineering problems such as ship design and ship handling.

## THE DYNAMICS CHARACTERISTICS OF SHAFTING SYSTEM

According to the construction features of ship propulsion system, the shafting can be simplified as a single disk system whose two ends are supported on the sliding bearing [6]. So, the mechanic model can be built as shown in Fig. 1.

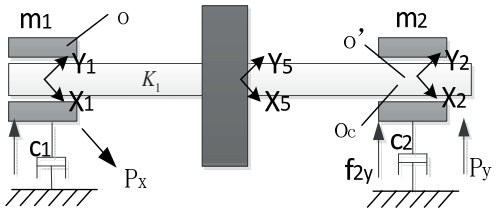


*Fig. 1. The mechanical model of shafting*

Furthermore, the model of single-disk motion can be obtained as shown in Fig. 2. The mass of disk is $m$ ; the moment of inertia is $J$ ; $o'(x, y)$ is coordinates of the geometric center of disk; $o_c(x_c, y_c)$ is the ordinates of mass center of disk; The eccentric distances of disk is $|o'o_c| = e$; The axis $\xi$ and the axis $\zeta$ are direction of the maximum and the minimum principal inertia axis of shaft. The $k_\xi, k_\xi$ is the maximum and the minimum elastic axis stiffness of shaft in the two axes direction.

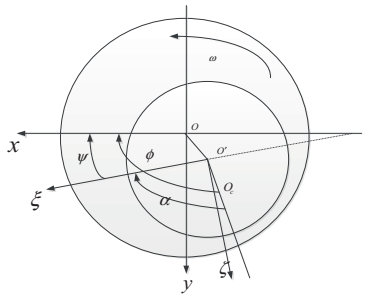


*Fig.2. The model of single-disk motion*

In the two coordinate systems of Fig.2, the coordinate correspondence can be expressed as following:

$$\begin{cases} x_c = x + e\cos\phi(t) \\ y_c = y + e\sin\phi(t) \end{cases} \tag{1}$$

In Eq. (1):

$\phi$ –the angle between x-axis and the line that linked the geometrical center and the mass center of disk, $\phi(t)$ is determined by the following geometric relations:

$$\phi(t) = \psi(t) + a = \int_0^t \omega dt + a \tag{2}$$

In Eq. (2):

$a$ – constant.

In normal operation, the rotational speed of shaft is constant. The disturbance loads can cause torsional vibration to the ship shafting, and then the flexural-torsional coupled resonance may occur.

The $\psi(t)$ can be expressed as follows:

$$\psi(t) = \omega t + \theta(t) \tag{3}$$

In Eq. (3):

$\theta$ – the distortion angle of shaft.

And then, the angular velocity and acceleration of disk can be expressed as follows:

$$\begin{cases} \phi(t) = \omega t + \theta + \alpha \\ \dot{\phi}(t) = \omega + \dot{\theta}(t) \\ \ddot{\phi}(t) = \ddot{\theta}(t) \end{cases} \tag{4}$$

The acceleration of the disc center of mass can be expressed as follows:

$$\begin{cases} \ddot{x}_c = \ddot{x} - e\ddot{\phi}\sin\phi - e\dot{\phi}^2\cos\phi \\ \ddot{y}_c = \ddot{y} + e\ddot{\phi}\cos\phi - e\dot{\phi}^2\sin\phi \end{cases} \tag{5}$$

The stiffness of propulsion shafting is associated with its principal axis of inertia and is a function that depends on the rotation angle [7]. The axis stiffness in the direction of both the maximum and minimum principal inertia axis is fixed, and the relationship between them can be expressed as:

$$\begin{pmatrix} k_x \\ k_y \end{pmatrix} = \begin{pmatrix} \cos^2\psi & \sin^2\psi \\ \sin^2\psi & \cos^2\psi \end{pmatrix} \begin{pmatrix} k_\xi \\ k_\zeta \end{pmatrix} = \begin{pmatrix} \cos^2(\phi-\alpha) & \sin^2(\phi-\alpha) \\ \sin^2(\phi-\alpha) & \cos^2(\phi-\alpha) \end{pmatrix} \begin{pmatrix} k_\xi \\ k_\zeta \end{pmatrix} \tag{6}$$

Due to the role of eccentric load, the rotary inertia force and gravity acted on the center of disc mass generate the rotational torque. Besides, there are other torque acted on the geometric center of the disc axle that are the torsion restore torque, torsional resistance torque, and the output torque of driving motor $M$. So, the moment equilibrium equations of the torsional vibration can be established as following:

$$\begin{aligned}(\mathrm{J}+\mathrm{me}^2)\ddot{\phi} &= me\ddot{x}\sin\phi - \\ m(\ddot{y}+g)e\cos\dot{\phi} &- k_n\theta + M\end{aligned} \tag{7}$$

Moreover, the dynamics equation of shafting-oil film-stern structure system[4] can be expressed as follows:

$$M\ddot{u} + (C+G)\dot{u} + Ku = F \tag{8}$$

In Eq. (8), the following parameters are:
– the mass matrix;
$u$ – the matrix of center coordinates;
$G$ – the matrix of the gyro;
$C$ – the damping matrix;
$K$ – the stiffness matrix;
$F$ – loads matrix.

According to the above dynamics equation, the motion equations of the disk, the front and back journals can be established as follows:

$$\begin{aligned}
&m_1\ddot{X}_1 + c_1\dot{X}_1 + k_1(X_1 - X_2) = f_{1X} + P_{1x} \\
&m_1\ddot{Y}_1 + c_1\dot{Y}_1 + k_1(Y_1 - Y_2) = f_{1Y} + P_{1y} - m_1 g \\
&m_2\ddot{X}_2 + c_1\dot{X}_2 + k_1(X_2 - X_1) + k_1(X_2 - X_5) = f_{2X} + P_{2X} \\
&m_2\ddot{Y}_2 + c_1\dot{Y}_2 + k_1(Y_2 - Y_1) + k_1(Y_2 - Y_5) = f_{2Y} + P_{2Y} - m_2 g \\
&m_5\ddot{X}_5 + c_5\dot{X}_5 + k_1(X_5 - X_2) = m_5 r\omega^2\cos\omega t \\
&m_5\ddot{Y}_5 + c_5\dot{Y}_5 + k_1(Y_5 - Y_2) = m_5 r\omega^2\sin\omega t - m_5 g
\end{aligned} \tag{9}$$

In Eq. (9):
$(X_1, Y_1)$ – the center coordinates of the front journal axis;
$(X_2, Y_2)$ – the center coordinates of the back journal axis;
$(X_5, Y_5)$ – the center coordinate of the disk with the eccentricity $r$;
$K_1$ – the elastic axis stiffness;
$k_c$ – the stern structure stiffness;
$f_{1x}$ – the oil film force of the left bearing;
$f_{1y}$ – the oil film force of the right bearing.

So, iterative calculation can be carried by solving simultaneous equations (8) and (9). In Eq. (8), the nonlinear oil film force can be calculated base on the working conditions of short bearing in which the influence of circumferential flow in bearing have be neglected.

## NUMERICAL SIMULATION OF RUB-IMPACT LOADS

According to the construction features of the ship shafting, When the rub-impact happen, the force acting point is on the center of disk mass [8]. The calculated mode of rub-impact loads can be obtained as shown in Figure 3.

Supposed the bearing deformation is small elastic deformation, the rub-impact force can be established as follows:

$$\begin{Bmatrix} P_x \\ P_y \end{Bmatrix} = -\frac{(e-\delta)k_c}{e}\begin{bmatrix} 1 & -f \\ f & 1 \end{bmatrix}\begin{Bmatrix} x \\ y \end{Bmatrix} \tag{14}$$

Where in:
$P_x$ – the radial component of the rub-impact force;
$P_y$ – the tangential component of the rub-impact force;
When $e < \delta$, both the radial force and tangential force are zero.
$\delta$ – the clearance between journal and bearing in the quiescent state;
$e$ – the tail bearing radius clearance, and $e = \sqrt{x^2 + y^2}$;
$k_c$ – the radial stiffness coefficient.
$f$ – the friction coefficient.

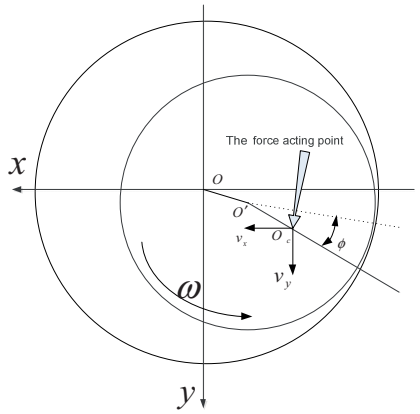


*Fig.3. The diagram of rub-impact force*

The numerical simulation can be carried by putting Eq. (14) in the Eq. (8) and (9). Initial parameters are set as: $m_1 = 100kg$, $m_2 = 80kg$, $m_3 = 200kg$, $c_1 = 5000N.S/M$, $K_1 = 5\times10^6 N/m$, $k_c = 5\times10^6 N/m$, $r = 0.06mm$, the radius clearance of bearing $\delta = 0.2mm$ [10]. The initial values of the system kinetics parameters, such as $\dot{X}_1$, $\ddot{X}_1$, $\dot{X}_2$, $\ddot{X}_2$, $\dot{X}_5$, $\ddot{X}_5$, $\ddot{Y}_1$, $\dot{Y}_1$, $\ddot{Y}_2$, $\dot{Y}_2$, $\dot{Y}_5$, $\ddot{Y}_5$, are taken as zero. Sensibility analysis results show that the change of initial value had no effect on calculation accuracy.

With the achievements by the former researchers, the condition of slight rubbing, continuous rubbing and severe rubbing can be obtained by setting the different speed to 500, 800, 900r/min [9]. Carrying out the integrative analysis, the center orbits curve and the amplitude-time response curve can be taken as shown in Figure 4~7, and the following conclusions can be drawn:

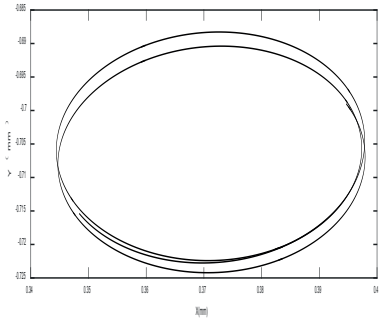

*Fig. 4. The center orbits under slight rubbing*

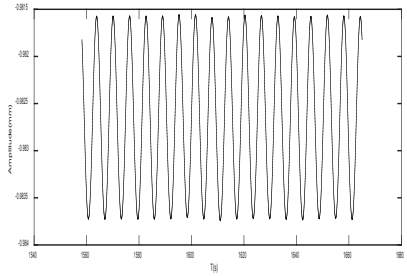

*Fig. 5. The torsional vibration amplitude under slight rubbing*

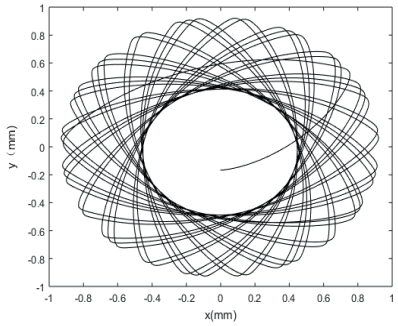


*Fig. 6. The center orbits under continuous rubbing*

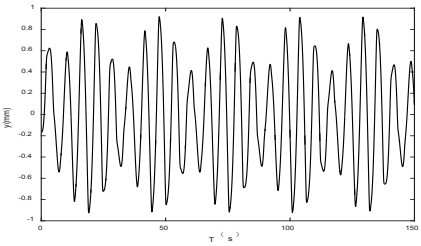


*Fig. 7. The torsional vibration amplitude under continuous rubbing*

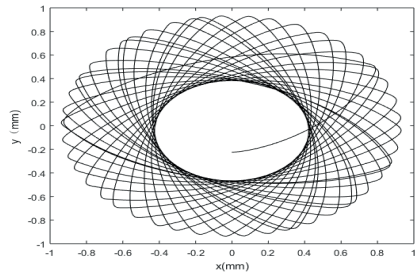


*Fig. 8. The center orbits under serious rubbing*

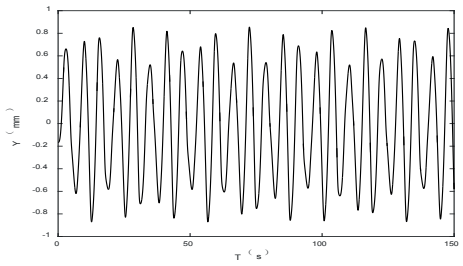


*Fig. 9. The torsional vibration amplitude under serious rubbing*

1. The rub-impact loads will disturb the motion of shafting bending vibration as show in Fig 4, 6 and 8. Under working conditions of slight rub-impact, the shaft can maintain the periodic motion and the center orbits of shafting is transient and cyclical as show in Fig 4 that the shaft is 4T cycle motion. When the rub-impact become serious, the instability of the system motion may result in almost periodic motion and chaotic motion as show in Fig 6 and 8 in which the frequency components of vibration include both low-frequency and high-frequency. And then, the center orbits of shaft under serious rubbing is more chaotic than that of continuous rubbing.

2. As shown in Fig.5, 7, 9, when shaft run under from the slight rubbing to the continuous rubbing, both the mode and the amplitude of torsional vibration change. In contrast, when the shaft run under from the continuous rubbing to the severe impact, the mode of torsional vibration change, the amplitude of torsion vibration almost remain unchanged.

It is obviously that rub-impact load had a real impact on torsional vibration. But the above conditions of rub-impact between the shaft and beraing require the shaft running at specific rotating speed. So, in order to obtain the law of torsional vibration in a wide variety of speed, it is necessary to simulate the working condition of rub-impact by experimental methods.

## THE TEST RIG WITH RUBBING GENERATOR

Considering the auxiliary shaft structure can be used to transfer the external loads [11], a test rig with an adjustable auxiliary shaft is established as shown in Fig. 10.

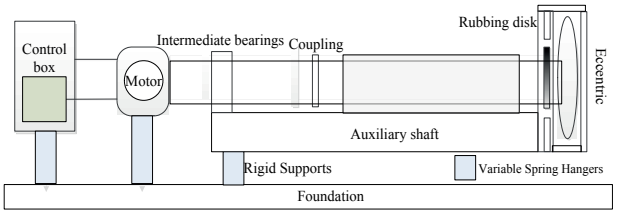


*Fig.10. The structure diagram of test rig*

In order to simulate the rub-impact load, a rubbing generator was attached to the test rig. The rubbing generator

produces various rub-impact loads that is transmitted to the auxiliary shaft and make it produce corresponding vibration and deformation. In the rig, the variable frequency motor is used to adjust the rotational speed of shafting, and the controlling and monitoring unit is applied to monitor the working condition of the shafting, and the force sensor are mounted on the bearing housing that can be used to obtain the force characteristic of the bearing oil film under different load conditions.

The rubbing generator with disk structuring is made of high quality carbon steel which can be installed and disassembled freely on the test rig [12]. Four adjustable bolts fixed on the rubbing generator under which is connected with the spring as shown in Fig. 11. When the length of bolts is adjusted, the rub-impact will happen sooner with certain gap between the journal and bearing. On the contrary, there is no gap in real state of rub-impact [13]. So, this test rig can simulate various rub-impact loads and is used to validate our model results and discussed later.

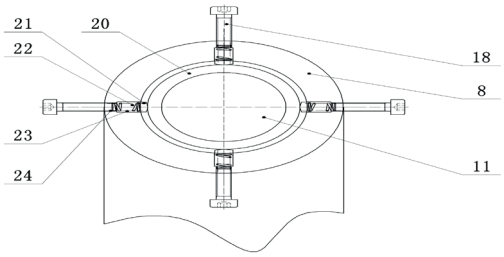


*Fig.11. The structure of rubbing generator*

Set the device stiffness $k_c = 10^5 N/m$, we test the reaction of the torsional amplitude to various rub-impact loads by measuring the maximum amplitude under different rotational speed. With the numerical simulation simultaneously, the observed value and the theoretical value are obtained as shown in Fig.12.

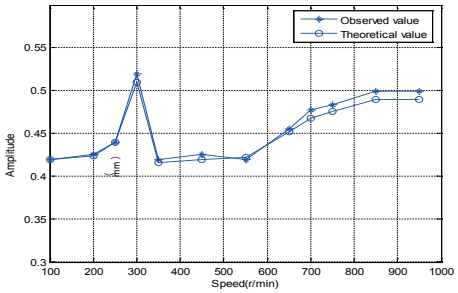


*Fig.12. The maximum amplitude with speed*

It can be see that the test rig and the real state had resemblance in the change regularities as shown that the observed value is accord with the theoretical value. When the shaft is at a lower speed and rub-impact haven't actually happened, the amplitude was in well keeping with the theoretical value. However, due to the gap between shaft and bearing under rub-impact loads in the test rig, both the continuous rubbing and severe rubbing are happening sooner rather than real state impact. Accordingly, the maximum amplitude of torsional vibration caused by the rub-impact load is slightly reduced rather than real state impact.

## RUB-IMPACT TEST BASED ON RUBBING GENERATOR

In order to evaluate the rub-impact condition of the test rig systematically, it is necessary to comparing the rules of change of maximum amplitude with the different rub-impact condition generated by rubbing generator [14].

In the experiment, the adjustment of rub-impact load is realized by adjusting the length of bolts or changing the spring stiffness of rubbing generator [15], that is changing the friction coefficient or elastic coefficient of rub-impact load. The condition of continuous rubbing and severe rubbing are obtained by choosing the speed to 700, 850r/min in Fig.12. And then, measuring the maximum amplitude at the front of the tail shaft under rub impact loads, the curve of the maximum amplitude with the friction coefficient and elastic coefficient can be taken as shown in Fig. 13 and 14. The experiment results show that the rub-impact loads affect ship shafting in a certain manner as follows:

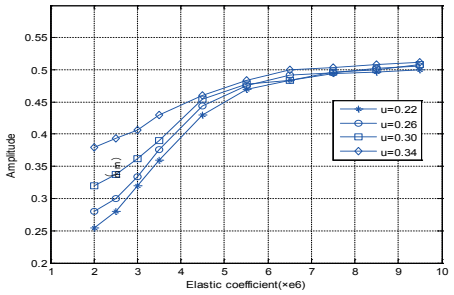


*Fig.13. The maximum amplitude under continuous rubbing*

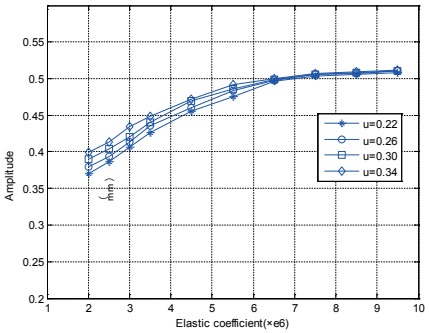


*Fig.14. The maximum amplitude under serious rubbing*

1. The rub-impact load had a real impact on torsional vibration under continuous rubbing than serious rubbing which is accord with the aforementioned theoretical analysis.

Furthermore, the biggest influence on torsional vibration under continuous rubbing is the friction coefficient, but that is elastic coefficient under serious rubbing.

2. When the coefficient of friction remained unchanged, the maximum amplitude of torsional vibration increases first fast and then slowly with the increase of elastic coefficients. The change speed of the maximum amplitude is different in different friction coefficients. As shown in Fig.14, the lower the friction coefficient is, the smaller the growth rate of the maximum amplitude is likely to be [16]. For example, when the friction coefficient is 0.22, the maximum amplitude has the fastest recovery speed which is not obvious when the coefficient is more than 0.34.

## CONCLUSION

In order to simulate the dynamic characteristics of ship shafting system under rub-impact load, the system mechanical model can be regarded as a single disk system whose two ends are supported on the sliding bearing. Furthermore, a test rig that can simulate the rub-impact load is built to carry out experimental verification. The results of the numerical simulation and experiments are summarized as follows:

1. The rub-impact loads will disturb the motion of ship shafting with compromise in both torsion vibration and bending vibration. However, on the voyage, the influence of rub-impact loads to the shafting torsion vibration is not obvious except in special working conditions that can be simulated by test rig with rubbing generator. The rubbing generator has provided useful research methods for the torsional vibration characteristics of shafting under various rubbing loads.
2. The maximum amplitude of torsional vibration increases with the increasing of both the friction coefficient and elastic coefficient in different manners. According to the influences model respectively under continuous rubbing or serious rubbing, the rub-impact loads response on shafting can be weaken by adjusting the radial and tangential rigidity of stern bearing.
3. Due to the clearance between shaft and bearing in the test rig have exert an influence on the rub-impact loads response, there is still a certain difference in the working condition between rub-impact generated by rubbing generator and the actual rub-impact [17], so further studies on rub-impact loads response of ship shafting are necessary.


### ACKNOWLEDGEMENTS

This research was supported by Zhejiang Provincial Natural Science Foundation of China under Grant No. LY16E090003.


### REFERENCE DOCUMENTS


1. DONG L X, YANG Y, GAO J K, et al. Response mechanism of impact load based on marine shafting-oil film-stern structure system [J]. Chinese Journal of Ship Research, Vol. 12, no. 1, pp. 122-127, 2017.
2. YANG L K. Study on the lubrication and rub-impact characteristics of stern bearing of ship [D]. Wuhan University of Technology, 2010.
3. LI H. Dynamic characteristics and fault analysis of RUB-impact rotor system [D]. North China Electric Power University,2016.
4. ZHU Li, PANG Fu-zhen, WANG Xue-ren, etl. Coupled Vibration Mechanism of Equipment and Ship Hull Structure[J]. Journal of Ship Mechanics, Vol. 17, no. 6, pp. 680-688, 2013.
5. Zhang C, Tian Z, Yan, X P. Analytical analysis of the vibration of propulsion shaft under hull deformation excitations [J]. Journal of Vibroengineering, Vol. 18, no. 1, pp. 44-55, 2016.
6. MA Hui, YANG Jian, SONG Rong-ze, NAI Hai-qiang, etl. Review and prospect on the research of rub-impact experiment of rotor systems [J]. Journal of Vibration and Shock, Vol. 33, no. 6, pp. 1-12, 2014.
7. X.F. Wen, Q. Yuan, J. S. Lu, et al. Analysis of Propulsion Shafting Torsional Vibration of Vessels with Double Engines and Double Propellers[C]. 3rd International Conference on Manufacturing and Engineering, pp. 1423-1428, 2012.
8. PAUL S. The Interaction between diesel engine, ship and propeller during manouevring [D]. Netherlands: Technische Univereiteit Delft, 2005.
9. Lech Murawski. Shaft line alignment analysis taking ship construction flexibility and deformations into consideration[J]. Marine Structures, Vol.18, no.1, pp. 62-84, 2005.
10. Jung WooSohn, Seung-BokChoi, Heung SooKim. Vibration control of smart hull structure with optimally placed piezoelectric composite actuators[J]. International Journal of Mechanical Sciences, Vol.53, no.8, pp. 647-659, 2011.
11. Wilfried Schiffer. Advanced methods for static and dynamic shafting calculations [J]. Brodogradnja, Vol.58, no.2, pp. 115-122, 2007.
12. H. Hirani, M. Verma. Tribological study of elastomeric bearing for marine propeller shaft system[J]. Tribology international, Vol.42, no.2, pp.378 -390, 2009.
13. Z.G. Zhang, Z.Y. Zhang, X.C. Huang, et al. stability and transient dynamics of a propeller-shaft system as induced by nonlinear friction acting on bearing-shaft contact

interface[J]. Journal of sound and vibration, Vol.333, no.12, pp.2608-2630 2014.

14. S. Merz, R. Kinns, N. Kessissoglou. structural and acoustic responses of a submarine hull due to propeller forces[J]. Journal of sound and vibration, Vol.325, no.1, pp.266-286, 2009.

15. L. Della, Pietra, G. Adiletta. The squeeze film dam perover four decades of investigations Part I: Characteristics and operating features[J]. SAGE. The Shock and Vibration Dight, Vol.34, no.1, pp.3-26, 2002.

16. Zhao Wu. Investigations on detection model of large scale rotation shaft torsional vibration in precision heavy machinery [J]. International Asia Conference on Informatics in Control, Automation and Robotics, pp. 459-463, 2009.

17. PENU Cheng, DAVILA C, HOU G S. Vibration analysis and sensitivity analysis of stepped beams using singularity functions[J]. Journal of Structures, Vol.2014, no.5, pp. 1-13, 2014.

**CONTACT WITH THE AUTHORS**

**Liangxiong Dong, associate Prof. Dr.**
*email: dongliangxiong@163.com*
tel.: 18368097266
Zhejiang Ocean University
Zhoushan Zhejiang 316022
**China**